International Journal of Hybrid Information Technology
Vol. 10, No.1 (2017), pp. 199-214
http://dx.doi.org/10.14257/ijhit.2017.10.1.18

Comparative Study of ZnO/Fe_2O_3 Nanocomposite Sensitized with Natural Pigments for Dye Sensitized Solar Cell

Kebede Gamo Sebehanie

School of Materials Science and Engineering, Jimma institute of technology, Jimma University, Ethiopia
krootseba@gmail.com

Abstract

This thesis examine and compares the efficiency of DSSC sensitized with natural dye extracted from Euphorbia amygdaloides and opuntia Ficus indica plant and pure ZnO, ZnO- Fe_2O_3 and pure Fe_2O_3 nanocomposite. The study starts by selecting natural dyes that they have good absorption spectra in the visible range using the UV-Vis spectrophotometer the selected natural dyes were Euphorbia amygdaloides and opuntia Ficus indica. Nanocomposites semiconductor oxide starting from pure ZnO, 95%ZnO-5% Fe_2O_3, 90% ZnO-10% Fe_2O_3, 80% ZnO-20% Fe_2O_3, and pure Fe_2O_3 were prepared using co-precipitation method. Then the prepared semiconductor oxide particle sizes were estimated using XRD. The estimated size of the prepared nanoparticles were ZnO =39.84nm, 95%ZnO-5% Fe_2O_3=23.22nm, 90% ZnO-10% Fe_2O_3=32.44nm, 80% ZnO-20% Fe_2O_3=38.38nm and pure Fe2O3=35.47nm. Finally dye sensitized solar cells (DSSCs) had been assembled and characterized from each dye extracted, Euphorbia amygdaloides. (Using Ethanol) and opuntia Ficus indica (using water) and the prepared semiconductor metallic oxide. The current density-voltage characteristics in the dark and under white light illumination and also IPCE under monochromatic illuminations have been studied. Solar energy conversion efficiency (η) of the as-synthesized semiconductors sensitized by the natural dye (Euphorbia amygdaloides. and opuntia Ficus indica) was obtained in the following order ZnO>80% ZnO-20% Fe_2O_3>95%ZnO-5% Fe_2O_3>90% ZnO-10% Fe_2O_3> Fe_2O_3. From the ten devices assembled best device parameter was achieved by the ethanol extract of Euphorbia amygdaloides. and pure ZnO nanoparticle semiconductor. The result was JSC=0.3696mAcm-2, VOC =0.33V, FF = 0.31 and η=0.038.

Keywords*: Dye sensitized solar cell (DSSC); ZnO- Fe_2O_3 nanocomposite; Euphorbia amygdaloides; Opuntia Ficus indica; XRD and UV-visible spectra*

1. Introduction

During the past decade, dye-sensitized solar cells (DSSCs) have attracted much attention in comparison with commercial Si-based solar cells; dye-sensitized solar cell (DSSC) is a potential photovoltaic alternative owing to its low price, easy fabrication and suitability for large area production. It mimics photosynthetic process, in which the light absorption and charge separation occur at different mediums [1]. In DSSCs, nanocrystalline semiconductor film as a photoanode can provide enormous surface area for adsorbing the dye to ensure enough photon absorption, high electron injection as well as high conversion efficiency. An outline of the operation of DSSC is depicted in Figure 1. The dye molecule is excited from ground state (D^0) to excited state (D^*) by sunlight, rapidly injects an electron into the conduction band (C_B) of semiconductor porous film. The electrons in C_B arrive at the counter electrode through the external circuit, and reduce

ISSN: 1738-9968 IJHIT

the I_3 ions to I ions with the aid of Pt. Then, I ions donate electrons to dye cations to complete the cycle of dye regeneration.

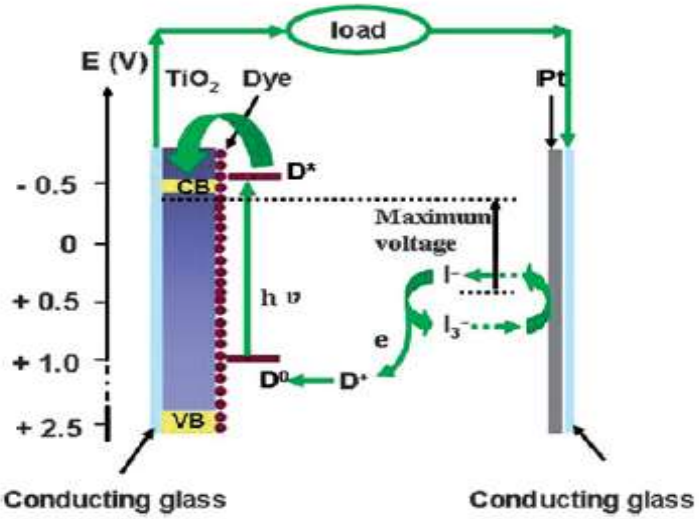

Figure 1. Schematic Illustration of the Working Principle of Dye-Sensitized Solar Cells [2]

1.1. Background

In 1976 Tsubomura *et al*. presented a working dye-sensitized porous zinc oxide photocell using a platinum counter electrode and an iodide/triidodie redox couple [3, 4]. In 1985, Desilvestro *et al*. used a rough TiO2 electrode sensitized with a ruthenium complex yielding enhanced photo conversion efficiency [5]. The breakthrough for DSSCs occurred in 1991, when Grätzel and O'Regan managed to build a 7.1%, photoelectrochemical device based on a dye-sensitized 10μm thick porous TiO2 electrode [6]. DSSC research has since then expanded and today there is a quite large research community trying to understand and improve the photovoltaic efficiency of the DSSCs. The record efficiency of a DSSC (single cell) has been reported to be 12% and had been presented in conferences in 2009 [7, 8 and 9].

Since then, extensive researches have continued to increase the power conversion efficiency (PCE) of DSSC by incorporating n-type metal oxide semiconductors such as TiO2, ZnO, SnO_2, Nb_2O_5, $SrTiO_3$ *etc*. and their composites as photoelectrode materials to achieve a reasonable efficiency of DSSCs of low cost, being therefore a promising alternative to conventional p-n junction solar cell. The wide band gap (E_g > 3eV) metal oxide semiconductors having suitable band position relative to sensitizer has been employed for the fabrication of DSSCs. The high surface area of nanoporous metal oxides facilitates the improvement of light absorption with improved dye loading for improved performance of DSSC. It is evident that the metal oxides employed for the fabrication of DSSCs has solar absorption below a threshold wavelength, λ_g (where, $\lambda_g = 1240/E_g$), *i.e.*, they have absorption at ultraviolet region. On the other hand, dye is only responsible for the absorption of light at visible and near-infrared region. The strong absorption of light is attributed to the intramolecular charge transfer transition (ICT) from electron donating group to the anchoring acceptor group of dye. Therefore, the anchored dye on to the metal-oxide surface helps the red shift of absorption threshold of metal oxide near infrared region (Rengaraj *et al.*, 2005). In addition to the above physical characteristics,

the inexpensiveness, natural abundance and facile synthesis methods of metal oxides and their composites is another advantage for the application in DSSCs.

Although most of the reported works on DSSC are based on TiO_2 porous thin films, various structures of ZnO are also being used for DSSC fabrication. The advantages of using ZnO over TiO_2 are its direct band gap (3.37 eV), higher exciton binding energy (60 meV) compared to TiO_2 (4 meV), and higher electron mobility (200 cm^2 V^{-1} s^{-1}) over TiO_2 (30 cm^2 V^{-1} s^{-1}). However, the efficiency of the DSSC based on ZnO nanostructures is still very low (5%).

Recently, considerable research on DSSCs has focused on improving the electron transport and reducing the re-combination rate by the use of alternative semiconductor materials or core-shell structures [10, 11]. In general, each TiO2nanoparticle is so small that it causes a problem in the formation of a space charge region [12–14], indicating that the recombination rate of the injected photoelectrons is very high due to the absence of an energy barrier at the electrode-to-electrolyte interface [15]. Tai and Bandaranayake *et al*. prepared a semiconductor composite, by using a chemical method, to reduce the recombination rate at the electrode-electrolyte interface [16, 17].

In addition, Nasr *et al*. prepared coupled semiconductor systems using several materials, such as ZnO/CdS TiO2/CdSe, SnO2/TiO2, and so on [18]. In this regards, an attempt to reduce the recombination rate with a bilayer of a metal-oxide semiconductors electrode is required for high-performance nanomaterial-based DSSCs.

1.2. Statement of the Problem

Perhaps the largest challenge for our global society is to find a way to replace the slowly but inevitably vanishing fossil fuel by renewable resources and at the same time avoid negative effects from the current energy system on climate, environment, and health. Among the alternative renewable energy source the DSSCs is one of best. The main problem of Dye sensitized solar cell (DSSC) is its efficiency that depends on different factor among these is; not able to absorb light in the broader region of the radiation from the sun.

1.3. Objective

The objective of this thesis is to compare the efficiencies of the DSSCs based on ZnO, Fe_2O_3 nanoparticles and ZnO/Fe_2O_3 (with different mass-mass ratio) nanocomposites sensitized with natural pigments and use it for solar energy conversion.

2. Experimental

2.1. Materials

In measuring the efficiency of dye synthesized solar cell, different materials were used; those materials and their uses are:- Electronic Digital balance to measure the mass of dye powder, flask for measuring the amounts of solvent used in the experiment, Drying materials (Compact 1300), magnetic stirrer to mix the solvent with the dye properly, centrifuge to separate the liquid dye from the residue, UV-Spectroscopy (UV-330) to measure the absorption spectra of the dye extracted from plants, Solvents such as Ethanol, Distilled water and 0.1M HCl and water for extraction of natural dyes from plant leaf, ITO glasses, Counter electrode and working electrode, to build the dye synthesized solar cell. Electrochemical analyzer with computer control (Model CHI-630A) without monochromator used to measure I-V curve and with monochromator to measure IPCE%, iodide/triiodide used as redox couple, lamp horizon (model 66182, ser. No 227, MFD11/94), sample holding, zinc acetate, nitrate nonahydrate, potassium hydroxide and chloroform used to extract ZnO and Fe_2O_3. XRD (BRUKER D8 Advance XRD, AXS

GMBH, Karisruhe, West Germany) to measure the average sizes of the synthesized nanocompsite semiconductor.

2.2. Methodology of the Study

Dyes were extracted from *Euphorbia amygdaloides*, *Hibiscus hypercum*, *Opuntia Ficus indica* and Syzgium guineense Plants using distilled water under acidic condition, ethanol and HCl. Measurements of absorption spectra were carried out by UV-visible spectrometer. And ZnO, Fe_2O_3 nanoparticles and ZnO-Fe_2O_3 nanocomposite with different percentage were synthesized and their average particles sizes were by characterizing with XRD. Then devices were fabricated using dye adsorbed ZnO-Fe_2O_3 film ITO electrodes and quasi solid state electrolytes PEDOT coated ITO as counter electrode finally investigate efficiency of the solar cell by radiating halogen display optic lamp with 100cm^{-2} then measuring fill factor (FF), short circuit current (I_{SC}), open circuit voltage (V_{OC}).

2.2.1. Synthesis of Pure Zinc Oxide (ZnO)

Pure zinc oxide (ZnO) was prepared by co-precipitation method using precursor zinc acetate dihydrate [(CH3 COO)2 Zn.2H2O] as follows measuring appropriate amount of zinc acetate and dissolving in distilled water then the salt was stirred until completely dissolved then slow (drop wise) addition of ammonium hydroxide (NH4OH) solution till pH was raised to 7 at which precipitation occurs. Stirring was continued for another 30min. after which the precipitate was aged for 24hrs, after drying for 1hr at 80 the content was vacuum filtered and the precipitate was calcined in three stages: stage I : 30min at 250℃ stage II : 30 min. at 600℃ and stage III : 1hr at 800℃.

2.2.2. Synthesis of Pure Iron Oxide (Fe_2O_3):

Pure iron oxide was prepared by co-precipitation method using precursor iron (III) nitrate nonahydrate, Fe (NO3)3.9H2O salt as follows measuring appropriate amount of iron (III) nitrate nonahydrate, and dissolving in distilled water then the salt was stirred until completely dissolved then slow (drop wise) addition of ammonium hydroxide (NH4OH) solution till pH was raised to 7 at which precipitation occurs. Stirring was continued for another 30min. after which the precipitate was aged for 24hrs, after drying for 1hr at 80 the content was vacuum filtered and the precipitate was calcined in three stages: stage I : 30min at 250℃ stage II : 30 min. at 600℃ and stage III : 1hr at 800℃.

2.2.3. Synthesis of Zinc-Iron (ZnO- Fe_2O_3) OXIDE NANOCOMPOSITE

Zinc-iron nanocomposite was prepared by co-precipitation method using, precursors, iron (III) nitrate nonahydrate, Fe (NO3)3.9H2O, zinc acetate dehydrate (CH3 COO)2 Zn.2H2O, and using zinc as host. Ammonium hydroxide, NH4OH, was used for precipitation and ethanol alcohol was employed to wash the precipitate. For this synthesis, appropriate amount of (CH3 COO)2 Zn.2H2O and Fe(NO3)3. 9H2O was used as salt precursors, starting with the pure zinc oxide at one end, continuing with different percentage of zinc-iron oxide nanocomposite and terminating at pure iron oxide at the other end. Aqueous solution of precursor salts were mixed and stirred for 30min. along with slow addition of NH4OH solution till pH was raised to 7 at which precipitation occurs. Stirring was continued for another 30min. after which the precipitate was aged for 24hrs, after drying for 1hr at 80 the content was vacuum filtered and the precipitate was calcined in three stages: stage I : 30min at 250℃ stage II : 30 min. at 600℃ and stage III : 1hr at 800℃ , step calcining was aimed to avoid thermal shock to samples.

2.2.4. Extraction of Natural Dye

The plant leaf, flower, and fruit were collected and let it to dry on clean place and open air (at room temperature). The dried plant parts were separately grinded to powder and kept in plastic containers. For each plant we had used 1gm powdered plant added to 35ml of the following solvent, i.e. distilled water, ethanol, and distilled water under acidic condition (0.1M HCl). Finally UV- visible absorption spectra of the dye was measured using UV-visible spectroscopy.

Figure 2. *E. Amygdaloides Leaf* and *Opuntia Ficus Indica* Fruit then Soaked with Working Electrode in the Extracted Dye

2.2.5. X-Ray Diffraction (XRD) Study

X-ray diffraction patterns of as synthesized semiconductors were obtained using a BRUKER D8 Advance XRD, AXS GMBH, Karisruhe, West Germany X-ray diffractometer equipped with a Cu target for generating a Cu Kα radiation (wavelength 1.5406 Å). The measurements were made at room temperature and the accelerating voltage and the applied current were 40 kV, 30 mA, respectively. The instrument was operated under step scan type with step time and degree (2θ) of 1s and 0.020°, respectively for the range of 4° to 64°.

2.2.6. Preparation of Working Electrode (WE)

The working electrode was prepared with different nanoporous like ZnO, Fe_2O_3 and with different proportion of ZnO-Fe_2O_3 nanocomposite placed on conducting glass and only separated by a thin layer of electrolyte solution (Acetonitrile) from the counter electrode. The prepared working electrode was soaked in the dye extracted from *opuntia Ficus indica and Euphorbia amygdaloides* plant. Then the dye was chemisorbed onto the ZnO, Fe_2O_3 and ZnO-Fe_2O_3 surface. (Figure 2).

2.2.7. Preparation of Counter Electrode (CE)

A CHI630 Electrochemical Analyzer and a three-electrode electrochemical cell were used for polymerization of EDOT. The poly(3, 4 – ethylene-dioxythiophene) (PEDOT) film for the counter electrode was formed by electrochemical polymerization of 3, 4-ethylenedioxythiophene (EDOT), in a three electrode one-compartment electrochemical cell. The electrochemical cell consisted of a pre cleaned ITO-coated glass working

electrode, platinum foil counter electrode and quasi-Ag/AgCl reference electrode dipped in (C2H5)4NBF4 acetonitrile solution. The solution used for the polymerization contained 0.1 M EDOT and 0.1 M (C2H5)4NBF4 in acetonitrile. The monomer was used as receiver. The polymerization was carried out potentiostatically at +1.8 V for 20 seconds. At this potential, the electrode surface becomes covered with blue-doped PEDOT film. Then the film was rinsed with acetonitrile and dried in air.

2.2.8. Preparation of Quasi Solid State Electrolyte

Quasi solid state electrolyte were prepared by 0.9 M of 1-ethyl -3- methyl immidazolium iodide (EMImI) was added into Acetonitrile under starring to form homogenous liquid electrolyte. In order to obtain better conductivity 0.5 M sodium iodide was dissolved in the above homogenous liquid electrolyte and then 0.12 M iodide and 3.5 % w/w of polyvinylpyrrolidone (PVP) were added. Then the resulting mixture was heated at 70 – 80°C under vigorous stirring to dissolve the PVP polymer, followed by cooling down to room temperature to form a gel electrolyte.

3. Results and Discussion

3.1. Absorption Spectra of Dyes Extracted from Plants

From the previous chapter we said that dye was extracted from different plant leaf *and* fruit. Their absorption spectra were measured then the one that has absorption spectra in the longer wave length were selected and also the one that had been extracted with distilled water was selected because ZnO will dissolve easily with acidic medium. The sunlight spectra contain much energy in the blue green area, which is the reason why the search is focused on red and purple dyes anthocyanins and betalains. Natural dye compounds generally contain anthocyanin, chlorophyll and Betalains. Anthocyanin has peak absorption at a wavelength of 500nm and 560nm. Chlorophyll is the pigment that is effective as a photosensitizer in the process of photosynthesis of green plants which has a maximum absorption at a wavelength of 670 nm and chlorophyll absorbs mostly blue and red, reflecting green. The absorption spectrums of chlorophyll–a and chlorophyll–b have two main absorption wave bands at 400-500 nm and 600-700nm respectively.

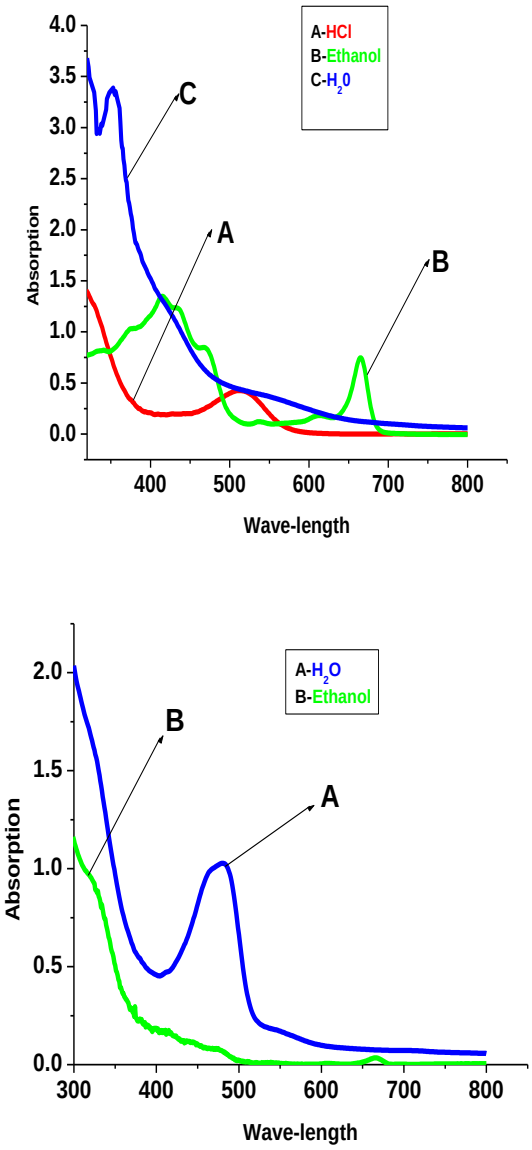

Figure 3. 1 UV –Vis Absorption Spectrum of *E. amygdaloides* (left) and *Opuntia Ficus indica* (right)

E. amygdaloides plant extracted in 0.1M HCl absorbance maximum peak is observed at wavelength $\lambda = 515$nm which shows the content of anthocyanin and when extracted with ethanol peak is observed at $\lambda = 666$ nm which shows the content of chlorophyll–b. When extracted with water there is no peak which shows that the nature of the dye is not soluble in water.

Opuntia Ficus indica extracted in water absorbance maximum peak is observed at wavelength $\lambda = 481$ nm which shows the content of Betalains. There is no absorption peak when it extracted with Ethanol which shows the nature of the dye is not soluble in Ethanol.

3.2. UV-visible Absorption Spectra of the Semiconductor Oxide

The prepared nanocomposites were first dispersed in distilled water and then the UV-Vis optical absorption characteristics of the nanocomposites were measured.

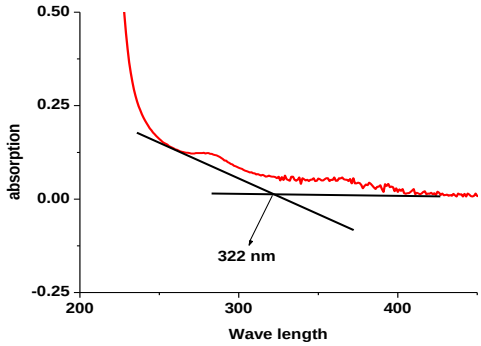

a. Pure zinc oxide

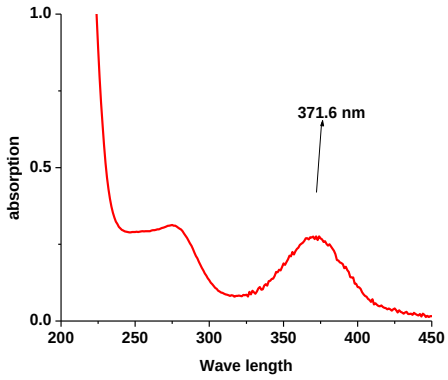

b. 95% ZnO-5%Fe_2O_3

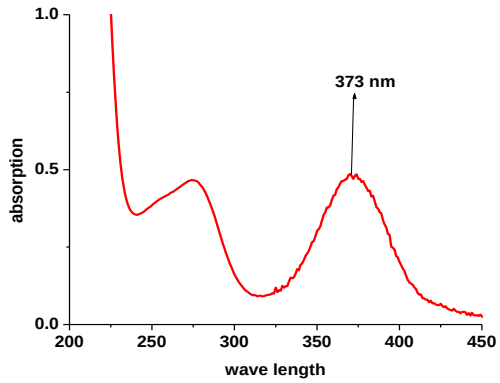

c. 90% ZnO-10%Fe_2O

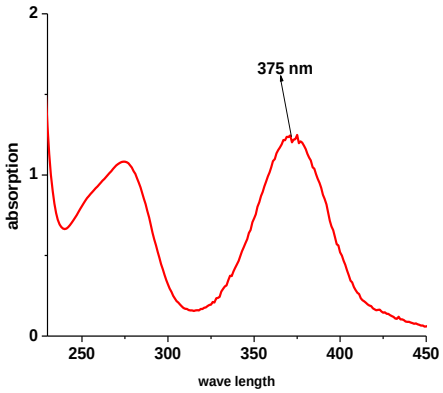

d. 80% ZnO-20%Fe_2O_3

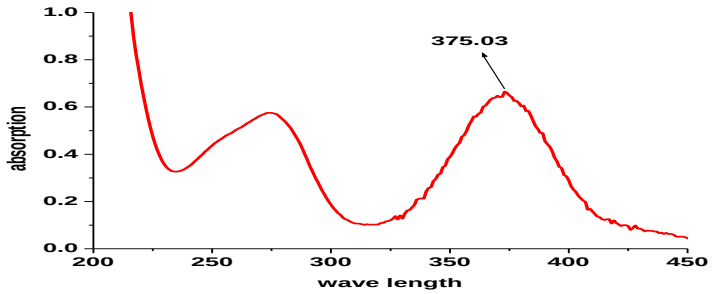

e. Pure Fe_2O_3

Figure (3.2a-3.2e). UV-visible Absorption Spectra of the Nanocomposites

From the above Figures 3.2(a-e) the absorption edges of the binary oxides shift remarkably to the visible range relative to the pure ZnO. This shift depends on the amount of Fe_2O_3 incorporated. The observed absorptions were not attributed to the ZnO and Fe_2O_3 bandgap absorption but rather it was the additional sub bandgap absorptions. These sub bandgap absorption may arise from surface states of the ZnO-Fe_2O_3 materials. The surface states are surface localized electronic states within the material bandgap, involving complex species such as dangling bonds, defects and atoms adsorbed on the surface [19].

Band gap energy (E_g) of the as-synthesized powders was calculated using Equation (1) [20].

$$E_g = \frac{1240\ eV}{\lambda_{max}} \quad (1)$$

Where, E_g is bandgap energy in electron volts and λ_{max} is the maximum wavelength (nm) corresponding to absorption edge.

Table 3.1. Maximum Wavelength and Energy Bandgap of the as – Synthesized Nanocomposites

Semiconductor oxide (%)	λ_{max} (nm)	Band gap (E_g) (eV)
Pure ZnO	322.0	3.85
95%ZnO-5%Fe_2O_3	371.6	3.33
90%ZnO-10%Fe_2O_3	373.0	3.32
80%ZnO-20%Fe_2O_3	374.8	3.30
Pure Fe_2O_3	375.1	3.30

3.3. XRD Analysis

X-ray powder diffraction of the synthesized nanocomposite powders: 100% ZnO, 95%ZnO-5% Fe_2O_3, 90% ZnO-10% Fe_2O_3, 80% ZnO-20% Fe_2O_3, and 100% Fe_2O_3 are shown in Figures 3.2 – 3.6. The average crystalline size was estimated using Dubye Scherere equation and given in Table 3.2.

$$D = \frac{K\lambda}{\beta \cos\theta} \quad (2)$$

Where:-

D: crystallite size in nm

K: the shape factor constant usually 0.9

β: the full width at half maximum (FWHM) in radians of 2θ

λ: the wave length of the X-ray which is 0.15406 nm for Cu target $K\alpha_1$ radiation and

θ: is the Bragg's angle

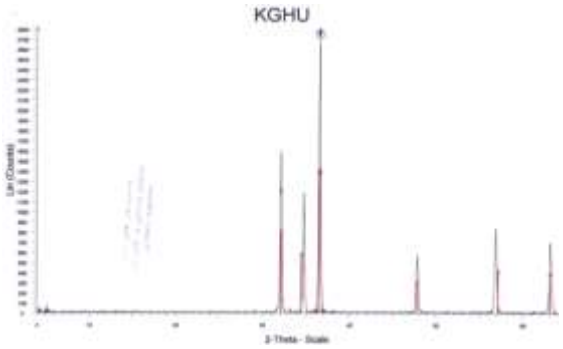

Figure 3.3. XRD Graph of 100% ZnO

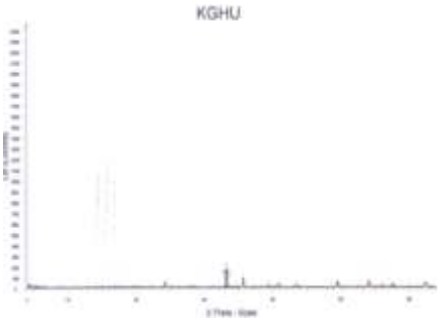

Figure 3.4. XRD Graph of 100% Fe_2O_3

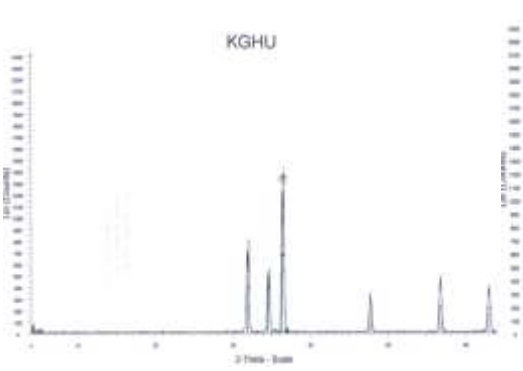

Figure 3.5. XRD Graph of 95% ZnO-5% Fe_2O_3

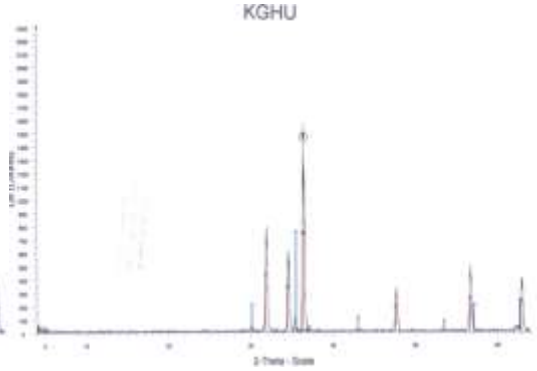

Figure 3.6. XRD Graph of 90% ZnO -10% Fe_2O_3

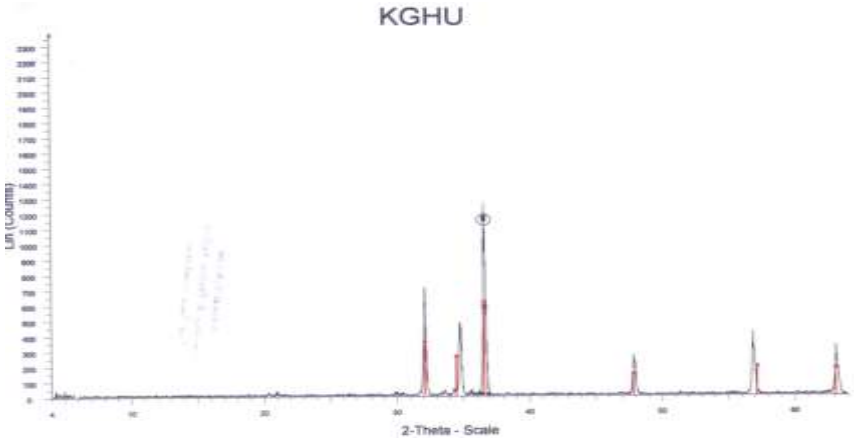

Figure 3.7. XRD Graph of 80% ZnO-20% Fe_2O_3

Table 3.2. Average Crystal Size of As-Synthesized Powder

Nano-composite	2θ degree	β(radians)	D(nm)
100% ZnO	36.7	0.00367	39.84
95% ZnO-5% Fe2O3	36.33	0.00628	23.22
90% ZnO-10% Fe2O3	36.45	0.00450	32.44
80% ZnO-20% Fe2O3	36.57	0.00380	32.44
100% Fe2O3	33.27	0.00408	38.39

3.4. Photoelectrochemical Properties of DSSCs Sensitized with Natural Dyes

The Photovoltaic test of a DSSC using these natural dyes as sensitizers were performed by measuring the current density–voltage (J–V) curves. The performance of natural dyes as sensitizers in DSSCs was evaluated by short circuit current J_{SC}, open circuit voltage V_{OC}, fill factor (FF), and power conversion efficiency (η). The Photoelectrochemical parameters of the DSSCs sensitized with natural dyes are listed in Table 3.3. For dyes that are extracted from ethanol and water.

3.4.1. Current Density-Voltage Characteristic

The current density-voltage characteristics of the *opuntia Ficus indica*, extracted by distilled water, and *E. amygdaloides*, extracted by Ethanol based on the five nanocomposite semiconductors with different proportion is shown in the Figure 3.7.

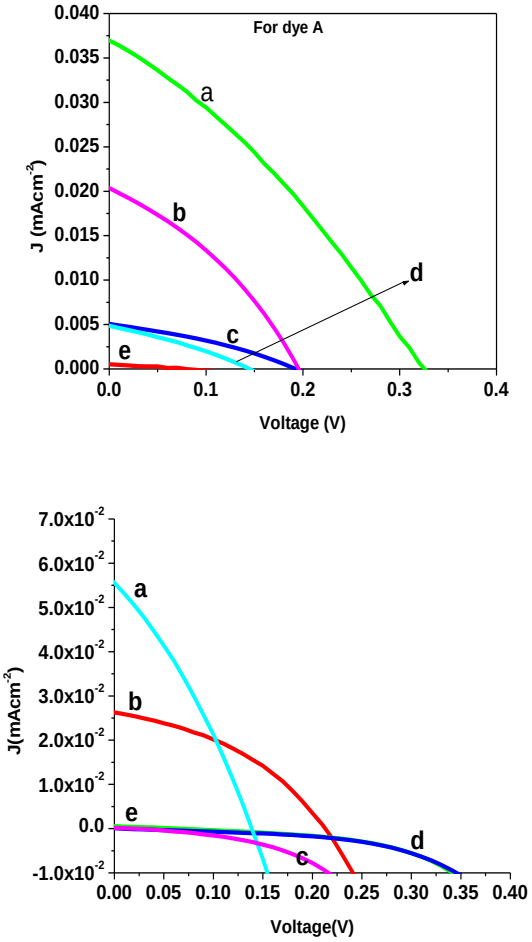

Figure 3.7. J-V curve based on a) pure ZnO, b) 80%ZnO- 20%Fe_2O_3 c) 95%ZnO- 5%Fe_2O_3 d) 90%ZnO- 10%Fe_2O_3 and e) pure Fe_2O_3 Sensitized with Natural Dye *Euphorbia amygdaloides*(left) and *opuntia Ficus indica (right)*

As we can see from the above Figure 3.7 the current density decreases with increasing the amount of concentration of Fe_2O_3 but at 80% ZnO-20% Fe_2O_3 it tends to increase for both types of dyes one probable reason may be when the concentration of iron oxide is small it tends to be surface as recombination center for the charge carrier rather than charge separation but at 80% ZnO-20% Fe_2O_3 probably it may co-sensitize with ZnO.

Table 3.3. Summary of the Short Circuit Current, Open Circuit Voltage, Fill Factor and the Efficiency of the Device Using the Semiconductor Oxide and the Selected Dyes

sensitizing dye	Semiconductor oxide	J_{SC}	V_{OC}	FF	η
Euphorbia amygdaloides	100% ZnO	0.3696	0.33	0.31	0.038
	95% ZnO-5% Fe_2O_3	0.00506	0.2	0.3204	0.0003242
	90% ZnO-10% Fe_2O_3	0.00486	0.15	0.294	0.0002143
	80% ZnO-20% Fe_2O_3	0.02035	0.2	0.3342	0.00136
	100% Fe_2O_3	5.32E(-4)	0.08	0.323	0.0000137
opuntia Ficus indica	100% ZnO	0.02624	0.22	0.38	0.0022
	95% ZnO-5% Fe_2O_3	5.564E(4)	0.07	0.264	0.0000103
	90% ZnO-10% Fe_2O_3	2.61E(-4)	0.06	0.52	0.000008
	80% ZnO-20% Fe_2O_3	0.05552	0.14	0.31	0.0024096
	100% Fe_2O_3	0.00165	0.08	0.314	0.0000414

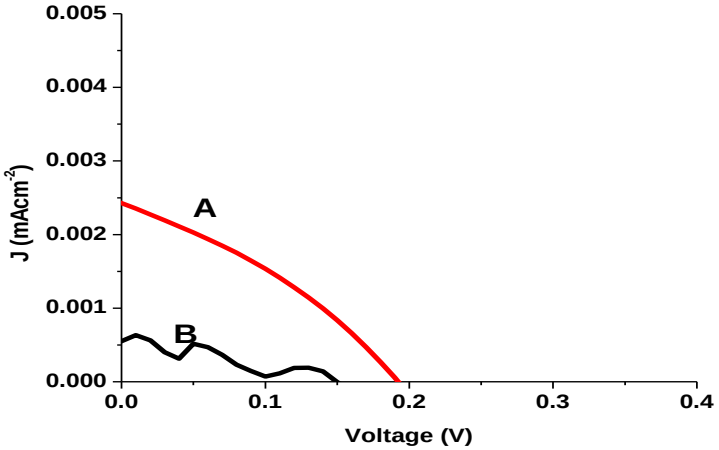

Figure 3.8. Comparisons of the J-V Characteristics based on Fe_2O_3 in DSSC when Using Dye and Without Using Dye

From Figure 3.8 we can see that J-V characteristics of the DSSC using dye (Figure 3.8A) and without using dye (Figure 3.8B). From this graph we can say that Fe_2O_3 sensitizing that means it can act as a dye.

3.4.2. Photocurrent Action Spectra

The incident monochromatic photon to current conversion efficiency (IPCE), defined as the number of electrons generated by light in the external circuit divided by the number of incident photons at each wavelength.

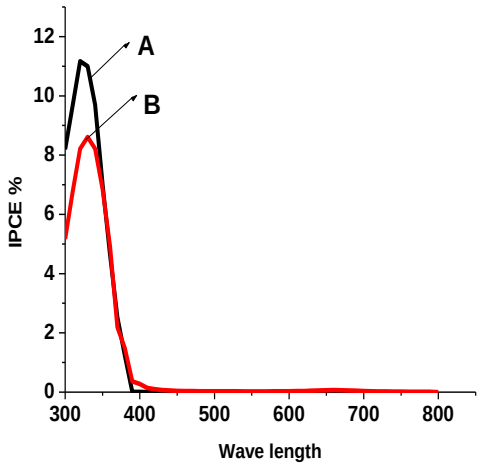

a. Pure ZnO

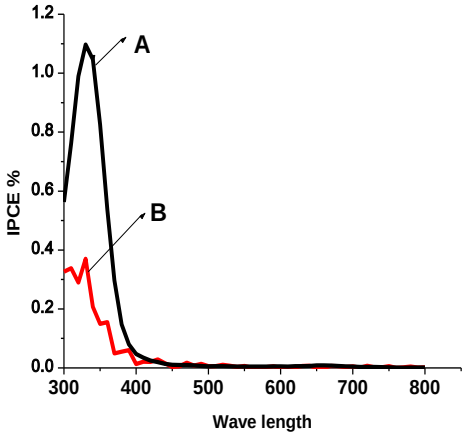

b. 95%ZnO-5%Fe_2O_3

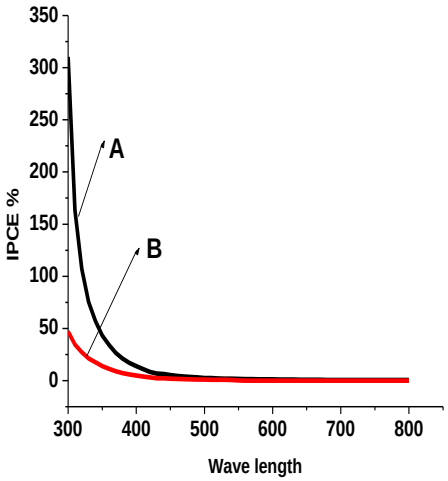

c 80%ZnO-20%Fe_2O_3

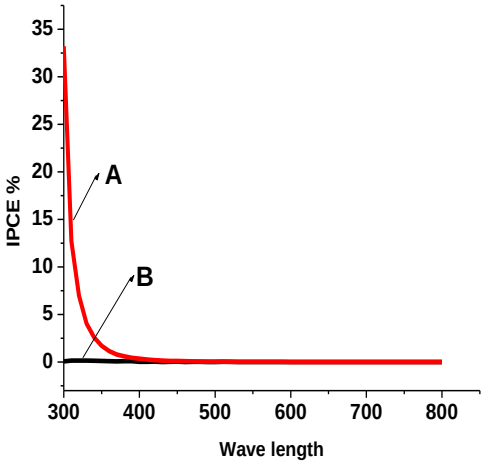

d. pure Fe_2O_3

Figure (3.9a-3.9d). IPCE % Vs Wave Length of the Different Semiconductor Oxide Sensitized with Opuntia Ficus Indica *(A)* and *Euphorbia* Amygdaloide (B)

The following Figures (3.9a -3.9d) shows the incident photon to current conversion efficiency (IPCE) spectra of 100% ZnO, 95%ZnO-5% Fe_2O_3, 80% ZnO-20% Fe_2O_3, and 100% Fe_2O_3 electrodes sensitized with *Euphorbia amygdaloide* and *opuntia Ficus indica* natural dyes as a function of wavelength.

From the graph we see that pure ZnO sensitized with *opuntia Ficus indica* and *Euphorbia amygdaloide* shows maximum IPCE in the ultraviolet region the rest didn't show and the result was 10.98%, which indicates the Zinc Oxide is more significance than the natural dye because there was no IPCE maximum in the visible region and the other suggestion may be the Fe_2O_3 was acting as recombination center. It is obvious that natural

dyes are very little effect on the performance of DSSCs rather synthetic dyes like ruthenium based complex dyes have much better effect on the efficiency of DSSCs.

Table 3.4. Summary of the Maximum Absorbance Wave Length for each Dye and Maximum IPCE Wave Length of the Characterized Devices

Sensitizing dye	Semiconductor oxide	λ_{max} (dye)	λ_{max}(IPCE)	IPCE %
Euphorbia amygdaloides	100% ZnO	665.9 nm	330.8nm	8.6
	95% ZnO-5% Fe_2O_3		332.3nm	1.09
	90% ZnO-10% Fe_2O_3		320nm	-
	80% ZnO-20% Fe_2O_3		-	-
	100% Fe_2O_3		326nm	0.16
opuntia Ficus indica	100% ZnO	481nm	323.5nm	10.98
	95% ZnO-5% Fe_2O_3		329.3nm	0.37
	90% ZnO-10% Fe_2O_3		-	-
	80% ZnO-20% Fe_2O_3		-	-
	100% Fe_2O_3		-	-

4. Conclusion

The objective of this research is to compare (study) the efficiencies of the DSSCs based on ZnO, FeO nanoparticles and ZnO/Fe_2O_3 (with different mass-mass ratio) nanocomposite sensitized with natural pigments. The obtained results can be summarized as follows.

XRD confirm the formation of nano-sized semiconductors of ZnO, Fe_2O_3 and ZnO/Fe_2O_3 nanocomposite. The efficiencies obtained were decreasing with increasing the concentration of Fe_2O_3. But at 80% ZnO-20% Fe_2O_3 the efficiency tends to increase even if the exact reason is unknown. The best efficiency obtained was with pure ZnO semiconductor oxide sensitized with *Euphorbia amygdaloides*, the short circuit current, the open circuit voltage, the fill factor and the efficiency are J_{SC}=0.3696, V_{OC} =0.33 , FF = 0.31 and η=0.038 respectively. Further investigation is needed at 80% ZnO-20% Fe_2O_3 nanocomposite because some strange thing is observed.

Acknowledgement

First and foremost, I would like to thank the almighty, **God**. Then I offer my deepest gratitude and respect to Dr. Sisay Tadesse for his unreserved support, excellent and generous guidance throughout my work. I gratefully acknowledge help from following organizations: Jimma Institute of technology, Hawassa University Physics department, Hawassa University Chemistry department, Addis Ababa University Chemistry Department, Geological Survey of Ethiopia (GSE).

References

[1] K. Lee, J. Kim, H. Kim, Y. Lee, Y. Tak, D. Kim and P.Schmuki, J. Korean Phys. Soc., vol. 54, **(2009)**, pp. 1027.
[2] B. O'Regan, D. T. Schwartz, S. M. Zakeeruddin and M. Grätzel, "Electrodeposited nanocomposite n–p heterojunctions for solid-state dye-sensitized photovoltaics", Adv. Mater, vol. 12, **(2000)**, pp. 1263–1267.
[3] K. R. J. Thomas, Y. C. Hsu, J. T. Lin, K. M. Lee, K. C. Ho, C. H. Lai, Y. M. Cheng and P. T. Chou, Chem. Mater, vol. 20, **(2008)**, pp. 1830-1840.
[4] H. Tsubomura, M. Matsumura, Y. Nomura and T. Amamiya, Nature, vol. 261, **(1976)**, pp. 402-403.
[5] J. Desilvestro, M. Gratzel L. Kavan, J. Moser and J. Augustynski, J. Am. Chem. Soc., vol. 107, **(1985)**, pp. 2988-2990.
[6] B. C. O'Regan and M. Gratzel, "A low-cost, high-efficiency solar cell based on dye-sensitized colloidal TiO2 films", Nature, vol. 335, **(1991)**, pp. 737–40.

[7] Y. Chiba, A. Islam, Y. Watanabe, R. Komiya, N. Koide and L. Han, "Dye-sensitized solar cells with conversion efficiency of 11.1%", Japanese Journal of Applied Physics,**(2006)**, vol. 45, pp. 638-640.
[8] M. K. Nazeeruddin, A. Kay, I. Rodicio, R. Humphry-Baker, E. Müller, P. Liska, N. Vlachopoulos and M. Graetzel, J. Am. Chem. Soc., vol.115, **(1993)**, pp. 6382-6390.
[9] B. Oregan and M. Gratzel, Nature, vol. 353, **(1991)**, pp. 737-740.
[10] A. Kay and M. Gratzel, Chem. Mater, vol.14, **(2002)**, pp. 2930
[11] E. Palomares, J. N. Clifford, S. A. Haque, T. Lutz and J. R. Durrant, J. Am. Chem. Soc., vol. 125, **(2003)**, pp. 475.
[12] A. Zaban, S. G. Chen, S. Chappel and B. A. Gregg, Chem. Commun., vol.134, **(2000)**, pp. 2231.
[13] D. Cahen, G. Hodes, M. Gratzel, J. F. Guillemoles and I. Riess, J. Phys. Chem. B, **(2000)**, vol. pp. 104, 2053.
[14] T. S. Kang, K. H. Chun, J. S. Hong, S. H. Moon and K. J. Kim, J. Electrochem. Soc., vol. 147, **(2000)**, pp. 3049.
[15] C. Bauer, G. Boschloo, E. Mukhtar and A. Hagfeldt, J.Phys. Chem., vol. 105, **(2001)**, pp. 5585.
[16] W. P. Tai, Sol. Energy Mater. Sol. Cells, **(2003)**, vol. 76, pp. 65.
[17] P. K. M. Bandaranayake, P. V. V. Jayaweera and K. Tennakone, Sol. Energy Mater. Sol. Cells, vol. 76, **(2003)**, pp. 57.
[18] C. Nasr, P. V. Kamat and S. Hotchandani, J. Elec-troanal. Chem., vol. 420, **(1997)**, pp. 201.
[19] A. Yella, H.-W. Lee, H. N, Tsao, C. Yi, A. K. Chandiran, M. K. Nazeeruddin, E. W.-G. Diau, Yeh, C.-Y. Zakeeruddin and M. Grätzel, *Science*, vol. 334, **(2011)**, pp. 629.
[20] K. G. Yaramahdi, W. Wijayantha, A. A. Tahir and B. Vaidhyanathan, *J. Phys. Chem. C.* vol.113, (**2009)**, pp. 4768.

